

# In-Silico Prediction of Phytoconstituents from *Manilkara Hexandra* for Antidiabetic Activity Targeting GKR (Glucokinase Regulatory Protein)

## Research Article

Apeksha P Motghare<sup>1</sup>, Parimal P Katolkar<sup>2\*</sup>, Tina S Lichade<sup>3</sup>

1. Department of Pharmaceutical Chemistry,  
Kamla Nehru College of Pharmacy, Butibori, Nagpur, Maharashtra, India.

### Abstract

**Objective:** A complex metabolic condition known as diabetes mellitus is caused by either inadequate or dysfunctional insulin. Once more, medicinal plants are being researched for the treatment of diabetes. Prototypical compounds found in medicinal plants have been the source of many conventional medications. The part of our investigation was to test the phytoconstituents of *Manilkara hexandra* for antidiabetic efficacy, *in-silico*. **Methods:** The pattern of interaction between the phytoconstituents from the *Manilkara hexandra* (Roxb.) Dubard, plant and the crystal structure of the antidiabetic proteins is evaluated using molecular docking in Discovery Studio (PDB ID: 4LY9). Later, SwissADME and pkCSM were used to screen for toxicity as well as the pharmacokinetic profile. **Results:** The docked results suggest that quercetin (-9.3 kcal/mol), kaempferol (-9.1 kcal/mol), *p*-coumaric acid (-6.4 kcal/mol) and cinnamic acid (-6.3 kcal/mol) for 4LY9 macromolecule has best binding towards antidiabetic activity as compared to the standard drug metformin (-5.0 kcal/mol). According to ADMET tests, pharmacokinetics and toxicity characteristics were also within acceptable bounds. **Conclusion:** Results from the binding potential of phytoconstituents aimed at antidiabetic activity were encouraging. It promotes the usage of *Manilkara hexandra* and offers crucial details on pharmaceutical research and clinical care.

**Key Words:** In-silico, *Manilkara hexandra*, Antidiabetic Activity, 4LY9, Discovery studio.

### Introduction

*Manilkara hexandra* (Roxb.) Dubard, synonym: *Mimusops hexandra* Roxb, is a plant that may be found all over central India and the Deccan Peninsula. It is grown throughout India's main geographical regions. It is also contrasted with *Khirni*. The fruit of the plant is one of the least used fruits in the state of Gujarat. It is frequently called Rayan. (1)

It is native to India and is mainly seen growing untamed in the south and north of the nation. Among the significant phytoconstituents identified are protobasic acid, 16-hydroxyprotobasic acid, taraxerol, triterpene ketone, alpha and beta-amyrin, cinnamates, alpha-spinasterol, beta-sitosterol, its beta-D-glucoside, quercetin, and its dihydroderivatives, ursolic acid. Traditional uses for the entire plant include astringency, aphrodisiac activity, alexipharmic effects, stomachic and anthelmintic properties, as well as relief from fever, flatulence, colic, dyspepsia, helminthiasis, hyperdipsia, and burning sensation. All of these compounds claimed

to have a variety of pharmacological effects, such as antioxidant effects. (2)

Chronic hyperglycemia, which is a hallmark of a group of metabolic diseases collectively known as diabetes mellitus, is brought on by deficits in insulin secretion, insulin action, or both. The importance of insulin as an anabolic hormone results in abnormalities in the metabolism of proteins, lipids, and carbohydrates. These metabolic abnormalities are caused by insulin resistance of target tissues, primarily skeletal muscles, adipose tissue, and to a lesser extent, liver, at the level of insulin receptors, signal transduction system, and/or effector enzymes or genes, as well as insufficient insulin levels to produce an adequate response. The intensity of symptoms depends on the kind and duration of diabetes. Patients with diabetes may experience blurred vision, weight loss, polydipsia, polyphagia, and polyuria. Some diabetic individuals don't exhibit any symptoms, especially those with type 2 diabetes who are still in the early stages of the disease. These symptoms, however, can also be present in patients with extreme hyperglycemia and, more so in children, those with complete insulin insufficiency. Uncontrolled diabetes can lead to coma, stupor, and, in rare instances, death from ketoacidosis or nonketotic hyperosmolar syndrome if it is not managed. (3-5)

A disruption of the crucial and intricate process of glucose homeostasis can result in hyperglycemia and type II diabetes mellitus. (6) In pancreatic b-cells, liver hepatocytes, certain hypothalamus neurons, and gut enterocytes, glucose is converted to glucose-6-

\* Corresponding Author:

**Parimal P Katolkar**

Department of Pharmaceutical Chemistry,  
Kamla Nehru College of Pharmacy, Butibori,  
Nagpur. 441108,  
Maharashtra, India.

Email Id: [parimal.katolkar@gmail.com](mailto:parimal.katolkar@gmail.com)

phosphate(7,8) by the important enzyme glucose kinase (GK), which controls glucose homeostasis. (9) In hepatocytes, GK controls glucose absorption, glycogen synthesis, and glucose production(10) while being inhibited by the naturally occurring GK regulatory protein (GKRP). (11–13) GK is removed from the gluconeogenic process and a fruitless cycle of glucose phosphorylation is avoided when GKRP binds to, inactivates, and sequesters GK in the nucleus during fasting. Blood glucose levels are reduced by substances that directly hyperactivate GK (GK activators), which are being studied in clinical trials as prospective therapies for the treatment of type II diabetes mellitus. (14,15)

However, there have only been a few studies on the phytoconstituents of *M. hexandra* that are used as an anti-diabetic. Molecular docking was employed in the current study to identify potential *M. hexandra* phytochemicals that are 4LY9-resistant while keeping in mind the data described above.

## Materials and methods

### Platform for molecular docking

A computational docking investigation of all the phytoconstituents selected as ligands with antidiabetic effect as the target was performed using the AutoDockVina software. (16)

### Protein preparation

A few phytoconstituents were analysed in-silico using the 2.00 crystal structure of the diabetes inhibitor (PDB ID:4LY9, resolution: 2.35, R-Value Free: 0.270, R-Value Work: 0.214, R-Value Observed: 0.217), which was obtained from the protein data bank (<https://www.rcsb.org>). Diabetes is treated with 4LY9. All extra molecules, including undesired chains, irregular residues, and co-crystallized water molecules, were removed using Discovery Studio. (17)

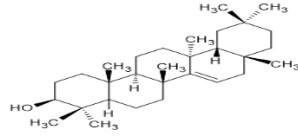

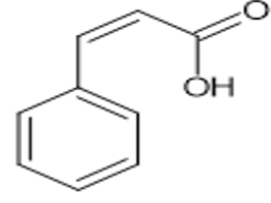
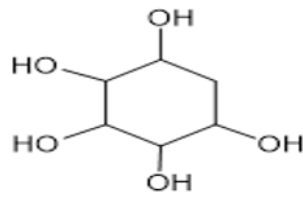
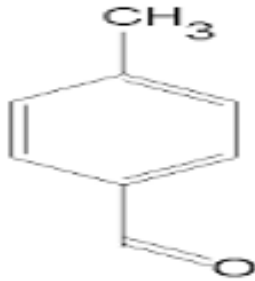
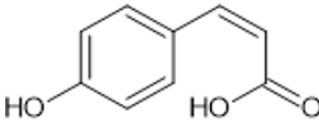
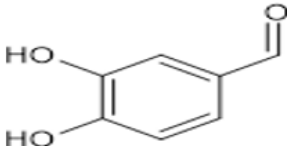
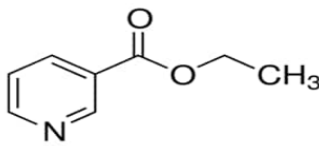
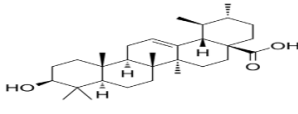
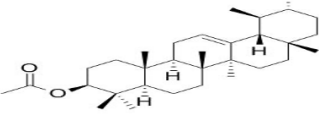
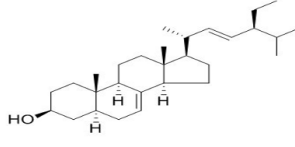
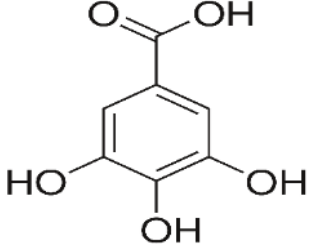
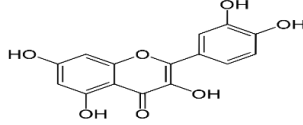
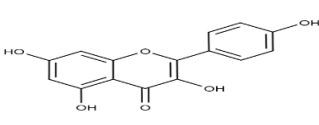
### Ligand preparation

Using the Avogadro programme, all constituents' three-dimensional (3D) structures were extracted from the PubChem database on the NCBI website (<https://pubchem.ncbi.nlm.nih.gov/>). However, the ChemSketch application was used to sketch the geometrical 2D structure. The ligand structures were saved in the PDB format and the two-dimensional (2D) structures were converted into 3D models using the Avogadro software. Figure 1 depicts each chemical structure.

### Molecular docking

Molecular docking examines the interactions between the protein and the ligand in order to establish the scoring function based on geometry and predict the binding affinity of the ligand molecule.(18,19) We investigated the interactions between particular phytoconstituents (Fig. 1), the common medicine, and the crystal structure of a macromolecule with antidiabetic activity using molecular docking techniques (PDB ID:4LY9). The molecular docking analysis was performed using PyRx software, and binding affinity was investigated using the Vina wizard tool. The final

**Fig. 1. Chemical structures of all selected phytoconstituents in the molecular docking studies**

<b>1. Taraxerol</b> 	<b>2. Hentriacontane</b> 
<b>3. Cinnamic acid</b> 	<b>4. Quercitol</b> 
<b>5. 4-Methyl benzaldehyde</b> 	<b>6. p-Coumaric acid</b> 
<b>7. 3,4-Dihydroxy benzaldehyde</b> 	<b>8. Ethyl nicotinate</b> 
<b>9. Ursolic acid</b> 	<b>10. α-Amyrin acetates</b> 
<b>11. α-Spinasterol</b> 	<b>12. Gallic Acid</b> 
<b>13. Quercetin</b> 	<b>14. Kaempferol</b> 

data was analysed and presented using Discovery Studio 2020 Client utilising bound ligands as the benchmark. (20) The protein-ligand interaction visualisation shows the number of interactions and active residues involved in substantial binding to the target enzyme's active site.

### Absorption, distribution, metabolism, and excretion (ADME) and toxicity prediction

Then, using Lipinski's rule, the selected phytoconstituents and the reference medicine were both evaluated for any potential drug-like properties. Prior to being taken by humans and animal models, phytochemicals must first be expected to be tolerable during the medicinal development phase. The pharmacokinetic profile (ADME) and toxicity predictions of ligands were determined using SwissADME (<http://www.swissadme.ch>) and pkCSM (an online server database predicting small-molecule pharmacokinetic properties using graph-based signatures, <http://biosig.unimelb.edu.au/pkcsm/prediction>). To study the toxicological properties of ligands, Simplified Molecular Input Line Entry System (SMILES) notations or PDB files were uploaded. Next, the necessary models were selected to produce a plethora of information about effects related to structure.(21,22)

### Standard Preparation

Metformin is the drug most frequently used for type 2 diabetes mellitus.(23)

Diabetes mellitus is a group of metabolic disorders characterised by inadequate insulin release or improper cell responses to insulin, both of which increase blood pressure. The resulting hyperglycemia results in serious complications. In people who are at high risk for developing diabetes, the drug metformin has been shown to significantly lower the majority of diabetic complications. Recent research on metformin not only reveals significant implications, such as reno-protective qualities, but some publications also imply its unfavourable effects, which are negligible when its favourable effects are taken into account.(24)

Avogadro Software is used to turn the 2D structure of the standard medicine into a 3D model, which is then saved in PDB format. Another example of how the standard is generated in stages is by first constructing the 2D structure of the standard medicine using the chemsketch tool. Molecular docking of metformin with 4LY9 was performed utilising PyRx.

## Results and Discussion

The current study's goal was to look into the phytoconstituents in *M. hexandra's* ability to hinder its antidiabetic action. For this work, we performed molecular docking studies using PyRx on all the phytoconstituents found in *M. hexandra*. The interactions between amino acid residues and their impact on the inhibitory potentials of the active ingredients were the subject of the following analysis. Selected phytoconstituents with the best match were

subsequently evaluated for their ADMET (absorption, distribution, metabolism, excretion, and toxicity) properties using the SwissADME and pkCSM servers.

### Molecular docking

Table 1 lists the docking rankings, binding energies, and interactions with amino acid residues of all the chemical components of *M. hexandra* that target antidiabetic activity (PDB ID: 4LY9).

**Table 1. Binding interaction of ligands from *M. hexandra* targeting antidiabetic activity (PDB ID: 4LY9)**

Sr. No.	Chemical constituent	PubChem ID	Docking Score 4LY9
1	Taraxerol	92097	-7.8
2	Hentriacontane	12410	-4.5
3	Cinnamic acid	444539	-6.3
4	Quercitol	441437	-5.8
5	4-Methyl benzaldehyde	7725	-5.5
6	<i>p</i> -Coumaric acid	322	-6.4
7	3,4-Dihydroxy benzaldehyde	8768	-6.0
8	Ethyl nicotinate	69188	-5.4
9	Ursolic acid	64945	-7.7
10	$\alpha$ -Amyrin acetates	92842	-8.6
11	$\alpha$ -Spinasterol	5281331	-7.1
12	Gallic acid	370	-6.5
13	Quercetin	5280343	-9.3
14	Kaempferol	5280863	-9.1
<b>Standard Drug</b>			
15	Metformin	4091	-5.0

The phytoconstituents had binding affinities for the 4LY9 macromolecule that ranged from -9.3 to -4.5 kcal/mol. From the docked results, it is clear that the compounds quercetin, kaempferol, *p*-coumaric acid, and cinnamic acid for 4LY9 exhibit the most favourable binding affinity (-9.3, -9.1, -6.4, and -6.3kcal/mol respectively) in complex with antidiabetic activity, as compared to other docked compounds, i.e., -amyrin acetates(-8.6 kcal/mol), taraxerol(-7.8 kcal/mol), ursolic acid(-7.7 kcal/mol),  $\alpha$ -spinasterol(-7.1 kcal/mol), gallic acid(-6.5 kcal/mol), 3,4-dihydroxy benzaldehyde(-6.0 kcal/mol), quercitol(-5.8 kcal/mol), 4-methyl benzaldehyde(-5.5 kcal/mol), ethyl nicotinate(-5.4 kcal/mol) and hentriacontane (-4.5 kcal/mol).

The standard's (metformin) binding affinity for 4LY9 is -5.0 kcal/mol.(25)

In addition, a study of the interactions between the ligand metformin and the 4LY9 protein complex revealed that the ligand molecule is oriented due to one salt bridge with GLU 32(A) amino acid, one unfavourable donor-donor bond with THR 31(A), one conventional hydrogen bond with GLY 181(A), one carbon hydrogen bond with LYS 514(A) and eight Van der Waals interactions with amino acid residues ARG 518(A), TRP 517(A), HIS 9(A), PRO 29(A), ARG 215(A), ASN 209(A), MET 213(A), SER 183(A) were also found.(Fig.2)

*Apeksha P Motghare et al., In-Silico Prediction of Phytoconstituents from Manilkara Hexandra for Antidiabetic Activity*

According to an examination of the interactions between the 4LY9 protein complex and the ligand quercetin. The ligand molecule is orientated as a result of three Pi-Alkyl interactions with ALA 27(A), VAL 28(A) and ARG 215(A), one unfavourable donor-donor interactions with ILE 11(A), four conventional hydrogen bonds with HIS 9(A), GLU 32(A), GLY 181(A) and TYR 24(A), and seven Van der Waals interaction with VAL 10(A), TRP 197(A), LYS 514(A), THR 31(A), SER 183(A), ASN 209(A), PRO 29(A) were also found. (Fig.3.a).

Additionally, an analysis of the interactions between the 4LY9 protein complex and the ligand kaempferol was carried out, and it was discovered that the ligand molecule is oriented as a result of two attractive charge interactions with ARG 478(A) and LYS 475(A), two conventional hydrogen bonds with THR 411(A), GLN 123(A), and seven Van der Waals interaction with GLN 474(A), LEU 338(A), THR 337(A), GLN 336(A), ASP 413(A), ASN 471(A), GLY 470(A) were also found. (Fig.3.b).

Additionally, an analysis of the interactions between the 4LY9 protein complex and the ligand, *p*-coumaric acid, was carried out. This analysis revealed that the ligand molecule is oriented as a result of one conventional hydrogen bond interaction with ASP 217(A), three attractive charge interaction with HIS 9(A), ARG 215(A) and TRP 517(A), two Pi-Alkyl interactions with VAL 10(A) and ALA 521(A), and four Van der Waals interactions with LEU 520(A), GLN 524(A), TYR 24(A) and LYS 514(A) were also found. (Fig.3.c).

Additionally, an analysis of the interactions between the 4LY9 protein complex and the ligand cinnamic acid was conducted, and it revealed that the ligand molecule is oriented as a result of one pi-cation interaction with GLU 32(A), three conventional hydrogen bond with THR 31(A), MET 213(A) and ASN 209(A), two Pi-Alkyl interaction with PRO 29(A), and LYS 514(A), and seven Van der Waals interactions with ARG 518(A), TRP 517(A), SER 183(A), GLY 181(A), ALA 214(A), LEU 182(A) and ARG 215(A) were also found. (Fig.3.d).

**Table 2. Binding interactions of ligands with the binding site of GKRP**

No.	Inhibitor	Binding energy (kcal/mol)	H bond	Main amino acid interactions	
				Pi-alkyl, Pi-sigma, alkyl, Pi-S/Pi-Pi stacking/Pi-Pi T-shaped/halogen/unfavourable donor-donor interactions	Van der Waals interaction
1	Taraxerol	-7.8	No Interaction	No Interaction	PHE 61(A), GLU 300(A), ALA 58(A), GLN 55(A), ARG 51(A), SER 310(A), GLY 54(A), TYR 307(A), GLN 304(A), HIS 303(A)
2	Hentriacontane	-4.5	No Interaction	LEU 52(A), ALA 58(A), LEU 37(A), PRO 36(A), PHE 61(A), HIS 303(A), ARG 301(A), ARG 297(A)	GLN 304(A), GLU 300(A), GLN 62(A), GLU 59(A), GLN 55(A), ALA 44(A), ASP 40(A)
3	Cinnamic acid	-6.3	THR 31(A), ASN 209(A), MET 213(A)	PRO 29(A), LYS 514(A), GLU 32(A)	ARG 518(A), TRP 517(A), SER 183(A), GLY 181(A), ALA 214(A), LEU 182(A), ARG 215(A)
4	Quercitol	-5.8	GLY 470(A), LYS 475(A), THR 411(A)	ARG 478(A)	GLN 336(A), ASP 414(A), ASP 413(A), HIS 438(A), LEU 338(A), GLN 474(A), ASN 471(A)
5	4-Methyl benzaldehyde	-5.5	ALA 521(A)	TYR 24(A), ILE 11(A), VAL 28(A), ALA 27(A)	VAL 10(A), GLN 524(A), TRP 517(A), LEU 520(A)
6	<i>p</i> -Coumaric acid	-6.4	ASP 217(A)	ALA 521(A), VAL 10(A), HIS 9(A), TRP 517(A), ARG 215(A)	LYS 514(A), LEU 520(A), TYR 24(A), GLN 524(A)
7	3,4-Dihydroxy benzaldehyde	-6.0	MET 213(A), GLY 181(A)	PRO 29(A), ARG 215(A)	ALA 214(A), ASN 209(A), THR 31(A), SER 183(A), GLU 32(A), ARG 518(A), LYS 514(A), TRP 517(A)
8	Ethyl nicotinate	-5.4	GLN 524(A), HIS 9(A)	ARG 518(A), LYS 514(A)	TRP 517(A), LEU 520(A), VAL 10(A), TYR 24(A), ALA 521(A), GLU 32(A)
9	Ursolic acid	-7.7	GLY 151(A)	ARG 149(A), HIS 565(A)	GLU 150(A), THR 152(A), SER 511(A), VAL 561(A), ASP 154(A), SER 558(A), GLN 562(A)
10	$\alpha$ -Amyrin acetates	-8.6	SER 310(A)	HIS 303(A), ALA 58(A)	PRO 311(A), ALA 314(A), GLU 47(A), VAL 50(A), ARG 51(A), TYR 307(A), GLY 54(A), GLN 304(A)
11	$\alpha$ -Spinasterol	-7.1	No Interaction	ARG 51(A), ALA 58(A)	TYR 307(A), SER 310(A), VAL 50(A), GLY 54(A), HIS 303(A), GLN 55(A), GLN 304(A), SER 308(A)
12	Gallic acid	-6.5	GLU 153(A), GLY 153(A), ARG 259(A)	SER 110(A), GLU 150(A), HIS 351(A)	ASN 512(A), LYS 514(A), GLY 108(A), ALA 184(A), SER 258(A), SER 257(A), MET 260(A), THR 109(A), THR 352(A)
13	Quercetin	-9.3	TYR 24(A), HIS 9(A), GLU 32(A), GLY 181(A), PRO 29(A), SER 183(A)	ILE 11(A), ALA 27(A), VAL 28(A), ARG 215(A)	VAL 10(A), TRP 517(A), LYS 514(A), THR 31(A), ASN 209(A)
14	Kaempferol	-9.1	THR 411(A), GLN 123(A)	ARG 478(A), LYS 475(A)	ASN 471(A), GLN 474(A), LEU 338(A), THR 337(A), GLN 336(A), GLY 470(A), ASP 413(A)
15	Metformin	-5.0	GLY 181(A), LYS 514(A)	GLU 32(A), THR 31(A)	SER 183(A), ASN 209(A), MET 213(A), ARG 215(A), PRO 29(A), HIS 9(A), TRP 517(A), ARG 518(A)

**ADMET study**

When a chemical is turned into an effective therapeutic, the pharmacokinetic profile (ADME) and toxicity predictions of the ligands require careful attention. These factors were evaluated in the current study utilizing SwissADME and pkCSM. The partition coefficient (Log P) and topological polar surface area (TPSA), which measure the absorption potential and lipophilicity, respectively. The TPSA should be less than 140 for a medication molecule to penetrate a cell membrane more effectively. Nevertheless, depending on the medication target, Log P's value varies. Intestinal and oral absorption should range from 1.35 to 1.80; sublingual absorption should be greater than 5, and central nervous system absorption should be greater than 5. (CNS). While the blood brain barrier (BBB) value falls between -3.0 and 1.2, the optimal range for

ligand solubility in water is between -6.5 and 0.5. (26) Drug resistance is also brought on by non-substrate P-glycoprotein. (27)

All of the chosen ligands in our investigation adhered to the P-glycoprotein non-inhibition TPSA criterion, demonstrating adequate intestinal absorption and a reasonable range of BBB values. All of the substances displayed range-acceptable aqueous solubility values. Additionally, it was projected that the chosen ligands would not exhibit skin sensitivity, hepatotoxicity, or AMES toxicity. It did not also inhibit hERG-I. (low risk of cardiac toxicity). Table 3 shows Lipinski's rule violations as well as the toxicity of *T. pyriformis*, minnows, the maximum tolerated dose, acute oral toxicity in rats, and chronic toxicity in rats. (28)

**Table 3. ADME and toxicity predicted profile of ligands with superior docking scores**

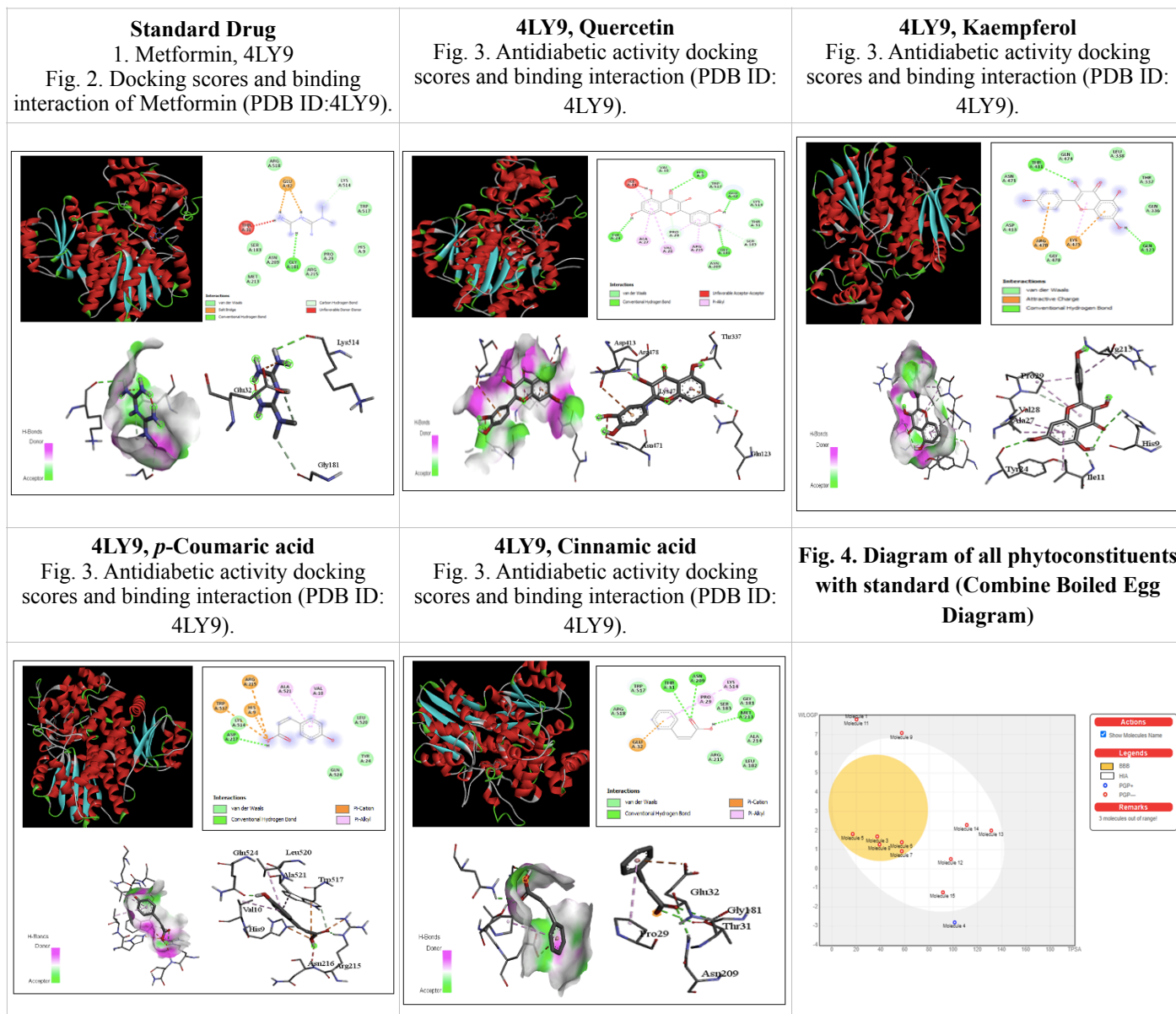
ADMET Properties	Formula	MW (g/mol)	Log P	TPSA (Å <sup>2</sup> )	HB donor	Hb acceptor	Aqueous solubility (Log mol/L)	Human intestinal absorption (%)	Blood-brain barrier
Taraxerol	C <sub>30</sub> H <sub>50</sub> O	426.72	8.17	20.23	1	1	-6.87	97.652	0.715
Hentriacontane	C <sub>31</sub> H <sub>64</sub>	436.84	12.34	0.00	0	0	-6.09	85.891	1.222
Cinnamic Acid	C <sub>9</sub> H <sub>8</sub> O <sub>2</sub>	148.16	1.68	37.30	1	2	0.65	94.35	-0.312
Quercitol	C <sub>6</sub> H <sub>12</sub> O <sub>5</sub>	164.16	-2.81	101.15	5	5	0.10	38.499	-1.082
4-Methyl Benzaldehyde	C <sub>8</sub> H <sub>8</sub> O	120.15	1.81	17.07	0	1	-1.71	97.33	0.394
<i>p</i> -Coumaric Acid	C <sub>9</sub> H <sub>8</sub> O <sub>3</sub>	164.16	1.38	57.53	2	3	-2.01	93.512	-0.184
3,4-Dihydroxy Benzaldehyde	C <sub>7</sub> H <sub>6</sub> O <sub>3</sub>	138.12	0.91	57.53	2	3	-0.75	77.745	-0.306
Ethyl Nicotinate	C <sub>8</sub> H <sub>9</sub> NO <sub>2</sub>	151.16	1.26	39.19	0	3	-0.75	98.458	-0.236
Ursolic Acid	C <sub>30</sub> H <sub>48</sub> O <sub>3</sub>	456.70	7.09	57.53	2	3	-4.65	97.503	-0.379
$\alpha$ -Amyrin Acetates	C <sub>32</sub> H <sub>52</sub> O <sub>2</sub>	468.75	8.60	26.30	0	2	-7.04	100	0.662
$\alpha$ -Spinasterol	C <sub>29</sub> H <sub>48</sub> O	412.69	7.80	20.23	1	1	-7.10	95.981	0.805
Gallic Acid	C <sub>7</sub> H <sub>6</sub> O <sub>5</sub>	170.12	0.50	97.99	4	5	-2.17	42.498	-0.958
Quercetin	C <sub>15</sub> H <sub>10</sub> O <sub>7</sub>	302.24	1.99	131.36	5	7	-3.13	69.235	-1.372
Kaempferol	C <sub>15</sub> H <sub>10</sub> O <sub>6</sub>	286.24	2.28	111.13	4	6	-3.30	74.567	-1.218
Metformin	C <sub>4</sub> H <sub>11</sub> N <sub>5</sub>	129.16	-1.03	88.99	4	2	-2.67	57.273	-1.117

**Table 3 Continued**

ADMET Properties	P-glycoprotein substrate	Total clearance [Log ml/(min.kg)]	Bioavailability score	AMES toxicity	Max tolerated dose [Log]	hERG I inhibitor	hERG II inhibitor
Taraxerol	NO	-0.081	0.55	NO	-0.066	NO	YES
Hentriacontane	NO	2.188	0.55	NO	-0.254	NO	YES
Cinnamic Acid	NO	0.869	0.85	NO	1.17	NO	NO
Quercitol	NO	0.595	0.55	NO	2.461	NO	NO
4-Methyl	NO	0.265	0.55	NO	1.121	NO	NO
<i>p</i> -Coumaric Acid	NO	0.682	0.85	NO	1.089	NO	NO
3,4-Dihydroxy Benzaldehyde	NO	0.552	0.55	NO	0.739	NO	NO
Ethyl Nicotinate	NO	0.782	0.55	NO	1.122	NO	NO
Ursolic Acid	YES	0.079	0.85	NO	-0.65	NO	NO
$\alpha$ -Amyrin Acetates	NO	0.029	0.55	NO	0.423	NO	YES
$\alpha$ -Spinasterol	NO	0.611	0.55	NO	-0.318	NO	YES
Gallic Acid	YES	0.527	0.56	NO	1.414	NO	NO
Quercetin	YES	0.502	0.55	NO	0.779	NO	NO
Kaempferol	YES	0.538	0.55	NO	0.935	NO	NO
Metformin	YES	0.332	0.55	YES	0.364	NO	NO

**Table 3 Continued**

ADMET Properties	Acute oral rat toxicity, LD50(mol/kg)	Oral rat chronic toxicity (Log mg/	Hepatotoxicity	Skin sensitisation	<i>T. Pyriformis</i> toxicity (Log µg/L)	Minnow toxicity (Log mmol/L)	Lipinski's rule violations
Taraxerol	2.828	1.288	NO	NO	0.41	-1.741	YES (1)
Hentriacontane	1.86	0.848	NO	YES	0.287	-5.021	YES (1)
Cinnamic Acid	2.05	2.549	NO	NO	-0.944	2.705	YES (0)
Quercitol	1.385	3.506	NO	NO	0.283	3.837	YES (0)
4-Methyl	1.731	1.959	NO	YES	-0.059	1.453	YES (0)
<i>p</i> -Coumaric Acid	1.912	2.953	NO	NO	0.223	1.79	YES (0)
3,4-Dihydroxy Benzaldehyde	1.865	2.149	NO	NO	-0.17	2.336	YES (0)
Ethyl Nicotinate	2.093	2.534	NO	YES	-0.39	2.187	YES (0)
Ursolic Acid	4.086	2.043	YES	NO	0.315	-0.596	YES (1)
$\alpha$ -Amyrin	2.261	2.187	NO	NO	0.37	-4.263	YES (1)
$\alpha$ -Spinasterol	2.454	1.125	NO	NO	0.56	-2.141	YES (1)
Gallic Acid	1.987	2.773	NO	NO	0.285	2.64	YES (0)
Quercetin	2.513	2.636	NO	NO	0.374	1.776	YES (0)
Kaempferol	2.329	2.616	NO	NO	0.448	1.034	YES (0)
Metformin	2.322	2.162	NO	YES	0.205	4.157	YES (0)



The ligand is shown in line and stick representation along with its 2D diagram and hydrogen bond interaction.

**Table 4. Names of molecules in a boiled egg diagram**

Molecule No.	Drug Name
1	Taraxerol
2	Hentriacontane
3	Cinnamic acid
4	Quercitol
5	4-methyl benzaldehyde
6	P-coumaric acid
7	3,4-dihydroxy benzaldehyde
8	Ethyl nicotinate
9	Ursolic acid
10	A-amyrin acetates
11	A-spinasterol
12	Gallic acid
13	Quercetin
14	Kaempferol
15	Metformin

Brain Or Intestinal Estimate permeation predictive model is abbreviated as **BOILED**.

Two zones, white and yellow, can be seen on the boiled egg diagram.

The yellow zone (yolk) represents the physicochemical space with the highest likelihood of molecules permeating to the brain, whereas the white region is the physicochemical space with the highest probability of molecules being absorbed via the gastrointestinal system.

Additionally, the spots are coloured red if they are anticipated to not be a P-gp substrate and blue if they are predicted to be actively effluxed by P-gp(PGP+) (PGP-).

Earlier, rats with normoglycemia and diabetic rats induced with alloxan were used to evaluate the effects of methanolic extracts of *Manilkara hexandra* on blood glucose levels. The results of this study supported the traditional usage of *Manilkara hexandra* in the treatment and/or control of type II diabetes. (29)

An analysis of the ethanolic extract of *Manilkara hexandra* bark's antidiabetic properties was done previously in streptozotocin-induced diabetes in experimental mice. According to the study's findings, 50% of the ethanolic extract exhibits considerable antidiabetic activity and a robust hypolipidemic potential in diabetic circumstances at various doses.(30)

This research backs up our *in-silico* research that suggests quercetin and kaempferol, which have the lowest binding energies (-9.3 kcal/mol and -9.1 kcal/mol, respectively) in complex with GGRP, may be useful in the treatment of diabetes. Regardless of the makeup of the phytoconstituents, the previously reported activity, however, is consistent with the extract's overall activity. Thus, it is clear from our work that the screened phytoconstituents had better interactions with the conserved catalytic residues, higher docking scores, and stronger binding energies, which resulted in the inhibition or blocking of the GGRP in diabetes. Our research thus offers convincing evidence that, among phytoconstituents, quercetin and

kaempferol have the greatest anti-cancer potential by specifically targeting GGRP.

## Conclusion

Hepatocytes generate the glucokinase regulatory protein (GGRP), also referred to as glucokinase (hexokinase) regulator (GCKR) (liver cells). Glucokinase (GK), a crucial enzyme in the metabolism of glucose, is controlled by GGRP's binding and movement of GK. In this study, we conducted an *in-silico* screening of *Manilkara hexandra's* phytoconstituents. In this work, fourteen compounds from chosen phytoconstituents were shown to have docking outcomes ranging from -9.3 to -4.5 kcal/mol. With the 4LY9 macromolecule, quercetin had the lowest binding energy of all the compounds (-9.3 kcal/mol), while metformin, the reference chemical, had the highest docking score with a binding energy of -5.0 kcal/mol.

In conclusion, phytoconstituents found in *Manilkara hexandra* have potent inhibitory effects on 4LY9 and may be further investigated for their potential to treat diabetes.

## References

- Bhutya RK: Ayurvedic Medicinal Plants of India. Scientific Publisher 2011.
- <https://ijpsr.com/bft-article/a-comprehensive-pharmacognostic-review-manilkara-hexandra-roxb-dubard/>
- American Diabetes Association. Diagnosis and classification of diabetes mellitus. Diabetes Care. 2014;37Suppl 1: S81–S90.
- Craig ME, Hattersley A, Donaghue KC. Definition, epidemiology and classification of diabetes in children and adolescents. Pediatr Diabetes. 2009;10Suppl 12:3–12.
- Galtier F. Definition, epidemiology, risk factors. Diabetes Metab. 2010; 36:628–651.
- Verspohl, E. J. Novel pharmacological approaches to the treatment of type 2 diabetes. Pharmacol. Rev. 64, 188–237 (2012).
- Agius, L. Glucokinase and molecular aspects of liver glycogen metabolism. Biochem. J. 414, 1–18 (2008).
- Matschinsky, F. M. Glucokinase as glucose sensor and metabolic signal generator in pancreatic beta-cells and hepatocytes. Diabetes 39, 647–652 (1990).
- Jetton, T. L. et al. Analysis of upstream glucokinase promoter activity in transgenic mice and identification of glucokinase in rare neuroendocrine cells in the brain and gut. J. Biol. Chem. 269, 3641–3654 (1994).
- Iynedjian, P.B.Mammalianglucokinase and its gene.Biochem. J.293,1–13 (1993).
- Van Schaftingen, E., Vandercammen, A., Detheux, M. & Davies, D. R. The regulatory protein of liver glucokinase. Adv. Enzyme Regul. 32, 133–148 (1992).
- Vandercammen, A. & Van Schaftingen, E. The mechanism by which rat liver glucokinase is

- inhibited by the regulatory protein. *Eur. J. Biochem.* 191, 483–489 (1990).
13. Anderka, O. et al. Biophysical characterization of the interaction between hepatic glucokinase and its regulatory protein: impact of physiological and pharmacological effectors. *J. Biol. Chem.* 283, 31333–31340 (2008).
  14. Coghlan M, Leighton B. Glucokinase activators in diabetes management. *Expert Opin. Investig. Drugs* 17, 145–167 (2008).
  15. Grimsby J, Berthel SJ, Sarabu R, Glucokinase activators for the potential treatment of type 2 diabetes. *Curr. Top. Med. Chem.* 8, 1524–1532 (2008).
  16. Morris G.M, Huey R, Lindstrom W, et al. AutoDock4 and AutoDockTools4: Automated docking with selective receptor flexibility, *Journal of Computational Chemistry*, 30 (16) (2009), pp. 2785-2791.
  17. Pettersen E.F, Goddard T.D, Huang C.C, et al. UCSF Chimera - a visualization system for exploratory research and analysis, *Journal of Computational Chemistry*, 25 (13) (2004), pp. 1605-1612.
  18. Verdonk M.L, Cole J.C, Hartshorn M.J, et al. Improved protein-ligand docking using GOLD, *Proteins: Structure, Function, and Bioinformatics*, 52 (4) (2003), pp. 609-623.
  19. Leach A.R, Shoichet B.K, Peishoff C.E, Prediction of protein-ligand interactions. Docking and scoring: Successes and gaps, *Journal of Medicinal Chemistry*, 49 (20) (2006), pp. 5851-5855.
  20. Biovia DS. Discovery studio modeling environment, Release 2017. San Diego: DassaultSystèmes, 2016.
  21. Arora S, Lohiya G, Moharir K, et al. Identification of potential flavonoid inhibitors of the SARS-CoV-2 main protease 6YNQ: a molecular docking study, *Digital Chinese Medicine*, 3 (4) (2020), pp. 239-248.
  22. Shah S, Chaple D, Arora S, et al. Exploring the active constituents of *Oroxylum indicum* in intervention of novel coronavirus (COVID-19) based on molecular docking method, *Network Modeling and Analysis in Health Informatics and Bioinformatics*, 10 (1) (2021), p. 8.
  23. Wang YW, He SJ, Feng X, Cheng J, Luo YT, Tian L, Huang Q. Metformin: a review of its potential indications. *Drug Des Devel Ther.* 2017 Aug 22;11: 2421-2429. doi: 10.2147/DDDT.S141675. PMID: 28860713; PMCID: PMC55.
  24. Nasri H, Rafieian-Kopaei M. Metformin: Current knowledge. *J Res Med Sci.* 2014 Jul;19(7):658-64. PMID: 25364368; PMCID: PMC4214027.
  25. Yende SR, Shah SK, Arora SK, Moharir KS, Lohiya GK. In silico prediction of phytoconstituents from *Ehretialaavis* targeting TNF- $\alpha$  in arthritis. *Digital Chinese Medicine.* 2021 Oct 1;4(3):180-90.
  26. Kaloni D, Chakraborty D, Tiwari A, Biswas S. In silico studies on the phytochemical components of *Murrayakoenigii* targeting TNF- $\alpha$  in rheumatoid arthritis. *Journal of Herbal Medicine.* 2020 Dec 1;24: 100396.
  27. Joshi T, Sharma P, Joshi T, Chandra S. In silico screening of anti-inflammatory compounds from Lichen by targeting cyclooxygenase-2. *Journal of Biomolecular Structure and Dynamics.* 2020 Aug 12;38(12):3544-62.
  28. Nisha CM, Kumar A, Vimal A, Bai BM, Pal D, Kumar A. Docking and ADMET prediction of few GSK-3 inhibitors divulges 6-bromoindirubin-3-oxime as a potential inhibitor. *Journal of Molecular Graphics and modelling.* 2016 Apr 1;65: 100-7.
  29. Nimbekar T.P., Katolkar P.P., Patil A.T. Effects of *Manilkara hexandra* on blood glucose levels of normal and Alloxan induced diabetic rats. *Research J. Pharm. and Tech.* 5(3): March 2012; Page 367-368.
  30. Das T, Das B, Saha D, Mishra SB. Anti-hyperglycemic activity of hydro-alcoholic bark extract of *Manilkara hexandra* (roxb) in streptozotocin induced diabetic rats. *Int. J. Pharm. Pharm. Sci.* 2016;8(4):1-4.

\*\*\*\*\*